Online Data Supplement

Methods

Experimental Animals and Tissue Collection

All protocols were approved by the Institutional Animal Care and Use Committee of the University of Texas Southwestern Medical Center. C57BL/6 mice (The Jackson Laboratory) were used for miRNA expression profiling during post-natal development. Neonatal mice (P0-P10) were euthanized by rapid decapitation with sharp surgical scissors. Older mice (P14-P84) were euthanized by CO_2 asphyxiation. For tissue collection, hearts were excised and immediately rinsed in phosphate-buffered saline (PBS), before being further dissected to remove non-cardiac tissue. For RNA analysis, atrial tissues were removed from ventricles (septum intact) and ventricles were blotted and weighed before snap-freezing in liquid nitrogen for storage at –80°C.

Generation of βMHC-miR-195 Transgenic Mice

A mouse genomic fragment flanking miR-195 was subcloned into a cardiac-specific expression plasmid containing 7 kb of upstream regulatory sequence from the βMHC promoter and human growth hormone poly(A)$^+$ signal.[1] Transgenic mice were generated by pronuclear injection using standard procedures. For genotyping, genomic tail DNA was isolated from mouse tail biopsies and analyzed by PCR using primers specific for the human growth hormone poly(A)$^+$ signal. βMHC-miR-195 transgenic mice were maintained on a mixed genetic background.

In Vivo Delivery of Synthetic LNA-antimiR Oligonucleotides to Neonatal Mice

Locked nucleic acid (LNA)-modified antimiRs directed against the mature miR-15b and miR-16 sequences were synthesized as unconjugated and fully phosphorothiolated oligonucleotides (miRagen Therapeutics, CO). The LNA-antimiRs were designed to perfectly complement 16 nucleotides of the mature miR-15b and miR-16 sequences, respectively (sequences shown in Online Table II). A control LNA-antimiR was also used, which contained the same LNA/DNA chemical composition as the anti-15/16 oligos, but was designed to target a miR sequence that is unique to *C. elegans* and is not expressed in mammals. Neonatal mice (CD-1/ICR strain, Charles River Laboratories) received control oligo, anti-miR-15b, anti-miR-16 or a combination of anti-miR-15b/16 at a dose of 25 mg/kg body weight via subcutaneous injection once per day at post-natal days 2, 3 and 4 (P2-P4). Hearts were harvested at P12 (i.e. 10 days after the first treatment) for assessment of miRNA knockdown, target gene regulation and histology.

Histological Analysis

Hearts used for histology were briefly rinsed in PBS, fixed in 4% paraformaldehyde overnight, and then transferred to 50% ethanol until paraffin embedding. Sections (5 μm thickness) were processed for H&E and Masson's trichrome staining according to standard procedures.

Immunofluorescence

All immunofluorescence was performed on paraffin sections as previously described.[2] The following primary antibodies were used: phospho-histone H3 (Ser10) (1:100, rabbit polyclonal, Millipore, MA), cardiac troponin T (1:100, mouse monoclonal, Thermo Scientific, IL), Aurora B (1:25, rabbit polyclonal, Sigma, MO) and wheat germ agglutinin conjugated to Alexa Fluor 594 (50 μg/ml, Invitrogen, CA). The following secondary antibodies were used: anti-mouse and anti-rabbit secondary antibodies conjugated to Alexa

Fluor 488 or 555 (1:400 dilution; Invitrogen, CA). Nuclei were identified by counter-staining sections with Hoechst 33342 (Invitrogen, CA).

For detection of apoptotic nuclei, paraffin sections were processed for immunofluorescent TUNEL staining using the *In Situ* Cell Death Detection Kit (TMR Red, Roche Applied Sciences, IN), according to the manufacturer's instructions.

RNA analysis

Total RNA was extracted from mouse hearts using TRIzol (Invitrogen). Quantitative real-time PCR was performed using an ABI 7000 cycler. cDNA was obtained by reverse transcription using random hexamers as primer (Invitrogen). SYBR green chemistry was employed for analysis of *Chek1*, *Cdc2a*, *Birc5*, *Nusap1* and *Spag5* mRNA expression levels, as previously described.[2] 18S ribosomal RNA and glyceraldehyde-3 phosphate dehydrogenase (GAPDH) were used as housekeeping controls. All primers for SYBR green reactions are listed in Online Table III. For detection of miRNA expression levels by real-time PCR, RT-PCR was performed using the TaqMan microRNA Reverse Transcriptase kit (Applied Biosystems, CA) and TaqMan probes (Applied Biosystems), according to the manufacturer's recommended protocol.

For detection of miRNAs by Northern blot, 20 μg of total RNA was loaded into each lane. RNA samples were run on 20% acrylamide denaturing gels and transferred to Zeta-probe GT genomic blotting membranes (Bio-Rad, CA) by electrophoresis. After transfer, membranes were UV cross-linked. Probes for miRNA detection were labeled with γ-^{32}P-ATP using T4 polynucleotide kinase (New England Biolabs, MA). Probes were hybridized to membranes overnight at 39ºC in Rapid-hyb buffer (Amersham Pharmacia). The following day, membranes were washed twice with 0.5x SSC containing 1% SDS at 39ºC for 15 min. Blots were exposed on film or by PhosphorImager analysis (GE HealthCare Life Sciences). A U6 probe served as a loading control for all blots. miRNA probe sequences for Northern blotting are provided in Online Table IV.

Microarray for miRNAs

miRNA profiling of P1 vs. P10 cardiac ventricles from C57BL/6 mice (n=3 per group) was performed using LC Science's miRNA microarray service (Chip ID = HM13.0). Details of sample preparation and analysis are as previously described.[3] A signal intensity cut-off of 500 was used with a P-value of less than 0.01 considered significant. This microarray chip comprised miRNA transcripts listed in Sanger miRBase Release 13.0.

Microarray for mRNAs

Microarray analysis was performed on RNA samples extracted from P1 cardiac ventricles from αMHC-miR-195 transgenic and wild-type mice.[4] Microarray analysis was performed by the University of Texas Southwestern Microarray Core Facility using the Mouse Genome 430 2.0 Array (Affymetrix, CA) as described.[5] A fold change cut-off of 1.5 was considered significant.

RISC RNA Sequencing

RISC RNA sequencing experiments were conducted on Argonaute 2 (Ago2) immunoprecipitates from P1 cardiac ventricles from αMHC-miR-195 transgenic and wild-type mice (n=3 WT and n=4 TG), as described previously.[6] Briefly, neonatal miR-195 transgenic and wild-type hearts were homogenized in lysis buffer containing yeast tRNA and SUPERnase-IN, as previously described.[6] Cardiac Ago2-associated RNA was immunoprecipitated using an anti-mouse Ago2 monoclonal antibody (Wako Pure) and TRIzol (Invitrogen) was subsequently added to the immunoprecipitated material to extract total RNA, as described.[6] Ago2-immunoprecipitated RNA was fragmented and processed for RNA sequencing (Illumina Genome Analyzer II, CA), as previously described.[6] Gene

expression values were expressed in terms of FPKM (fragments per million mapped reads). Fold enrichment scores were obtained for each gene by expressing the FPKM for a given transcript in miR-195 transgenic RISC relative to wild-type. A fold enrichment cut-off of greater than 2.0 was considered significant. MiR-15 family binding sites were identified in putative target transcripts by cross-referencing to three different computational algorithms for prediction of miRNA 3'UTR binding sites (TargetScan 5.1, miRanda 3.0 and PITA v6.0).

Gene Ontology Cluster Analysis

Gene ontology analysis was performed for genes that were significantly regulated in miR-195 transgenic hearts (>1.5-fold) and for genes that were enriched in miR-195 transgenic RISC (>2-fold). Gene ontology analysis was conducted using the Database for Annotation, Visualization, and Integrated Discovery (DAVID) functional annotation tool. DAVID analysis was performed with 'High' classification stringency and P-value cut-off of 0.001.

Embryonic and Neonatal Rat Cardiomyocyte Isolation

For embryonic and neonatal cardiomyocyte isolations, timed pregnant Sprague-Dawley rats (Harlan Laboratories) were ordered at E15.5 and harvested at E19, P1, P3, P7 and P14 for isolation of cardiomyocytes and RNA analysis. Ventricular cardiomyocytes were isolated by enzymatic digestion using the Neomyt isolation system for neonatal rat/mouse cardiomyocytes (Cellutron Life Technology, MD), according to the manufacturer's recommended protocol. Isolated cardiomyocytes were further purified with the use of tetramethyl rhodamine methyl ester (TMRM) (Invitrogen), a fluorescent probe which monitors the mitochondrial membrane potential that can be used to sort cells with high metabolic activity (e.g. cardiomyocytes).[7] Briefly, neonatal rat cardiomyocytes were incubated with 10 nmol/L TMRM at 37ºC for 30 minutes. TMRM-labeled cells were then trypsinized and immediately sorted by FACS (Moflo) at 488nm excitation wavelength to obtain a TMRM-high population of purified cardiomyocytes. To check cell purity, we performed immunocytochemical staining with an anti-sarcomeric alpha actinin antibody (Sigma), which indicated that >99% of the purified cells were cardiomyocytes. TMRM-sorted cardiomyocytes were snap-frozen in liquid nitrogen and RNA was extracted with TRIzol (Invitrogen) for miR-15 expression profiling by real-time PCR.

Primary Neonatal Cardiomyocyte Cultures and Adenoviral Infection

Neonatal rat cardiomyocytes were obtained from 1-3 day-old Sprague-Dawley rats (Harlan Laboratories) using the Neomyt isolation system for neonatal rat/mouse cardiomyocyte isolation (Cellutron Life Technology), as described above. Following fibroblast pre-plating, isolated cardiomyocytes were plated overnight onto gelatinized (Surecoat, Cellutron Life Technology) 24-well plates containing 35 mm laminin-coated glass cover slips (MatTek, MA) at a density of 0.125×10^6 cells/well. Neonatal cardiomyocytes were cultured overnight in DMEM/M199 media (4:1) supplemented with 10% horse serum, 5% fetal bovine serum, penicillin/streptomycin (100 units/ml), essential and non-essential vitamins (Gibco), essential amino acids (Gibco) and insulin-transferrin-sodium-selenite (ITSS) supplement (Boehringer Mannheim). Cultured myocytes were changed to serum-free media the following day. Twenty-four hours after culture in serum-free media, cardiomyocytes were infected with recombinant adenoviruses expressing either β-galactosidase (AdGal, control) or miR-195 (Ad195).[3] Forty-eight hours after viral infection, myocytes were either harvested for RNA analysis or processed for cell cycle profiling by flow cytometry (see below).

Cell Cycle Analysis by Flow Cytometry

Cell cycle analysis by flow cytometry of cells labeled with propidium iodide was performed as previously described,[8] with minor modifications. Briefly, cultured neonatal cardiomyocytes were dissociated with 0.25% trypsin/EDTA and spun down (1000 rpm for 5 minutes) to obtain a cell pellet. The cell pellet was washed with cold Ca^{2+}/Mg^{2+}-free PBS and resuspended in cold PBS to get a single cell suspension. Cells were fixed in ice cold 70%

ethanol for 45 minutes and spun down to obtain a cell pellet (2000 rpm for 10 minutes). Fixed cells were permeabilized (15 minutes, 0.5% Triton X-100 in PBS), incubated for 30 minutes in 1% BSA/PBS, and subsequently incubated for 45 minutes with an antibody to sarcomeric tropomyosin (diluted 1:1000 in 1% BSA/PBS, Sigma). After washing with 0.1% Nonidet P40 and 1% BSA/PBS, cells were incubated with an FITC-conjugated goat anti-mouse IgG antibody (diluted 1:500 in 0.5% Tween and 1% BSA/PBS; Dianova). Cells were then resuspended in propidium iodide staining solution (5 ng/ul propidium iodide, 1μg/ul RNase A, dossiolved in PBS). Cells were incubated in propidium iodide staining solution for 30 minutes at 37ºC and then immediately analyzed by flow cytometry and the distribution of cells in different cell cycle phases assessed by Flowjo software.

Cell Culture, Transfection and Luciferase Assays

A 1948-bp genomic fragment of the *Chek1* 3' UTR encompassing the miR-15 family binding site was PCR-amplified and ligated into the firefly luciferase (f-luc) reporter construct (pMIR-REPORTTM; Ambion) USING SpeI and HindIII sites (See Online Table V for primer sequences). The seed region of the miR-195 target site in the Chek1 3'UTR was mutated using the QuickChange II site-directed mutagenesis kit (Stratagene). A single-stranded miR-195 mimic containing five 3' and five 5' terminal 2'OMe residues was synthesized (Integrated DNA Technologies). COS cells were transfected with Lipofectamine 2000 (Invitrogen) according to manufacturer's instructions. Forty-eight hours after DNA/RNA transfection, cell extracts were assayed for luciferase expression, using the luciferase assay kit (Promega). Luciferase activity was expressed as luminescence relative units normalized to β-galactosidase expression in cell extracts.

References

1. Rindt H, Gulick J, Knotts S, Neumann J, Robbins J. In vivo analysis of the murine beta-myosin heavy chain gene promoter. *J Biol Chem* 1993;268:5332-5338.

2. Porrello ER, Mahmoud AI, Simpson E, Hill JA, Richardson JA, Olson EN, Sadek HA. Transient regenerative potential of the neonatal mouse heart. *Science* 2011;331:1078-1080.

3. van Rooij E, Sutherland LB, Thatcher JE, DiMaio JM, Naseem RH, Marshall WS, Hill JA, Olson EN. Dysregulation of microRNAs after myocardial infarction reveals a role of miR-29 in cardiac fibrosis. *Proc Natl Acad Sci U S A* 2008;105:13027-13032.

4. van Rooij E, Sutherland LB, Liu N, Williams AH, McAnally J, Gerard RD, Richardson JA, Olson EN. A signature pattern of stress-responsive microRNAs that can evoke cardiac hypertrophy and heart failure. *Proc Natl Acad Sci U S A* 2006;103:18255-18260.

5. Davis CA, Haberland M, Arnold MA, Sutherland LB, McDonald OG, Richardson JA, Childs G, Harris S, Owens GK, Olson EN. PRISM/PRDM6, a transcriptional repressor that promotes the proliferative gene program in smooth muscle cells. *Mol Cell Biol* 2006;26:2626-2636.

6. Matkovich SJ, Van Booven DJ, Eschenbacher WH, Dorn GW, 2nd. RISC RNA sequencing for context-specific identification of in vivo microRNA targets. *Circ Res* 2011;108:18-26.

7. Hattori F, Chen H, Yamashita H, Tohyama S, Satoh YS, Yuasa S, Li W, Yamakawa H, Tanaka T, Onitsuka T, Shimoji K, Ohno Y, Egashira T, Kaneda R, Murata M, Hidaka K, Morisaki T, Sasaki E, Suzuki T, Sano M, Makino S, Oikawa S, Fukuda K. Nongenetic method for purifying stem cell-derived cardiomyocytes. *Nat Methods* 2010;7:61-66.

8. Engel FB, Hauck L, Cardoso MC, Leonhardt H, Dietz R, von Harsdorf R. A mammalian myocardial cell-free system to study cell cycle reentry in terminally differentiated cardiomyocytes. *Circ Res* 1999;85:294-301.

Online Tables*:*

Online Table I: List of miRNAs significantly (P<0.01) regulated between P1 and P10.

MiRNA	Average P1 signal	Average P10 signal	Fold Change (P10/P1)
hsa-mir-195	387	4524	11.68992248
hsa-miR-100	326	2090	6.411042945
hsa-miR-150	137	724	5.284671533
mmu-miR-505	68	348	5.117647059
hsa-miR-146a	98	495	5.051020408
hsa-miR-15a	179	889	4.966480447
hsa-miR-486-3p	433	1771	4.090069284
hsa-miR-139-5p	178	582	3.269662921
hsa-let-7d*	576	1848	3.208333333
hsa-miR-99a	1024	3114	3.041015625
hsa-miR-148a	1354	3524	2.602658789
hsa-miR-486-5p	2492	5854	2.349117175
hsa-miR-152	1027	2320	2.259006816
mmu-miR-805	2470	5023	2.033603239
hsa-miR-15b	2788	5626	2.017934003
hsa-miR-27b	4100	8193	1.998292683
hsa-miR-125a-5p	6324	12191	1.92773561
hsa-let-7e	8117	15638	1.926573857
hsa-let-7b	11764	22273	1.893318599
hsa-miR-125b	10223	19271	1.885063093
hsa-miR-30b	9058	17052	1.882534776
hsa-miR-16	6182	11268	1.822711097
hsa-miR-199a-3p	5052	9086	1.798495645
hsa-miR-574-3p	276	470	1.702898551
hsa-miR-30a	4604	7824	1.699391833
hsa-miR-451	4811	8096	1.682810227
hsa-miR-130a	940	1504	1.6
hsa-miR-23a	12891	20601	1.598091692
hsa-miR-30e	1395	2202	1.578494624
hsa-miR-185	1032	1540	1.492248062
hsa-let-7g	11969	17678	1.476982204
hsa-miR-23b	15817	22230	1.405449832
hsa-miR-378	4771	6692	1.402640956
hsa-let-7c	19496	27232	1.396799343
hsa-let-7f	19697	26607	1.350814845
hsa-miR-151-5p	2708	3553	1.312038405
hsa-miR-24	6375	8219	1.289254902
hsa-miR-1979	8174	10478	1.281869342
hsa-miR-30c	15226	19269	1.265532642
hsa-miR-499-5p	8388	10113	1.20565093
hsa-let-7d	24489	27271	1.113602025
hsa-miR-103	3724	2758	0.740601504
hsa-miR-107	3686	2531	0.686652198
hsa-miR-20a	2768	1843	0.665823699
hsa-miR-1259	21741	13714	0.630789752

hsa-miR-23a	3586	2261	0.630507529
hsa-miR-329	10193	6369	0.624840577
hsa-miR1277	21668	13341	0.615700572
mmu-miR-329	33885	19529	0.57633171
hsa-miR-498	36637	20918	0.570952862
mmu-miR-667	195	105	0.538461538
mmu-mirR-322*	3706	1878	0.506745818
hsa-miR-1275	597	286	0.479061977
hsa-miR-433	385	177	0.45974026
mmu-miR-29b*	496	217	0.4375
hsa-miR-1469	1269	547	0.431048069
mmu-miR-705	4360	1834	0.420642202
hsa-miR-503	196	77	0.392857143
hsa-miR-941	59	23	0.389830508
mmu-miR-483	2493	941	0.377456879
hsa-miR-1268	1713	640	0.373613543
mmu-miR-762	9911	3333	0.336293008
hsa-miR-638	12252	3849	0.314152791
hsa-miR-940	255	77	0.301960784
mmu-miR-224	387	113	0.291989664
mmu-miR-290-5p	807	188	0.232961586
mmu-miR-351	6460	1366	0.211455108
hsa-miR-371-5p	2790	532	0.190681004
hsa-miR-208b	8513	1431	0.168095853
hsa-miR-220a	312	49	0.157051282
mmu-miR-689	5179	748	0.144429427

Online Table II: LNA-antimiR sequences for Anti-15 and Anti-16. d = DNA, l=LNA.

AntimiR	Sequence (l-LNA, d=DNA)
Anti-15b	5' lAs;dCs;dCs;lAs;lTs;dGs;lAs;lTs;dGs;lTs;lGs;dCs;dTs;lGs;dCs;lT 3'
Anti-16	5' lAs;dTs;dAs;lTs;lTs;dTs;lAs;lCs;dGs;lTs;lGs;dCs;dTs;lGs;dCs;lT 3'

Online Table III: List of primer sequences used for real-time PCR analysis.

Gene	NCBI Reference Sequence	Primer Sequences
Chek1	NM_007691.5	S 5'-GGGGTGGTTTATCTTCATGG-3' AS 5'-GCCAAGCCAAAGTCAGAGAT-3'
Cdc2a	NM_007659.3	S 5'-TCCGTCGTAACCTGTTGAGT-3' AS 5'-TGGCCAGTGACTCTGTGTCT-3'
Birc5	NM_009689.2	S 5'-TGGACAGACAGAGAGCCAAG-3' AS 5'-AGCTGCTCAATTGACTGACG-3'
Nusap1	NM_133851.3	S 5'- AATTTAGCCAAAAGGCTGGG-3' AS 5'- CCTTGTTTCTGGATTCAGGTG-3'
Spag5	NM_017407.2	S 5'- CTTTCCCACCAGCTACAAGC-3' AS 5'- GGTGTCTTAGTGACCCCACAA-3'

Online Table IV: miRNA probe sequences used for Northern blotting.

miRNA Probe	Sequence
miR-15a	5'-TGAGGCAGCACAGTATGGCCTG-3'
miR-15b	5'-TGTAAACCATGATGTGCTGCTA-3'
miR-16	5'-CGCCAATATTTACGTGCTGCTA-3'
miR-195	5'-GCCAATATTTCTGTGCTGCTA'3'
miR-497	5'-TACAAACCACAGTGTGCTGCTG-3'
let-7a	5'-AACTATACAACCTACTACCTCA-3'

Online Table V: Primer sequences used for cloning Chek1 3'UTR and for mutating the miR-15 family binding site within the Chek1 3'UTR (Chek1 3'UTR mut).

miRNA Probe	Sequence (restriction enzyme sites in bold)
Chek1 3'UTR sense	5'-**ACTAGT**GCTGTCAGCTCTGCACATTC-3'
Chek1 3'UTR antisense	5'-**AAGCTT**TGGTCAAGCCCTTGTGCAGC-3'
Chek1 3'UTR mut	5'-CTAGTGCACATTCCTGGTGAATAGAG-3'

Online Figure Legends:

Online Figure I: Genomic localization, conservation and sequence homology of miR-15 family members. A, Schematic showing the genomic organization of the miR-15a/16-1, miR-16b/16-2 and miR-195/497 clusters. Mammalian conservation is represented as a histogram. **B.** Sequences for the miR-15 family members miR15a/15b/16/195/497. The "seed" region is highlighted in red text.

Online Figure II: Tissue distribution and developmental regulation of miR-15 family members. A, Northern blot analysis of miR-15 family members across multiple adult tissues. **B,** Northern blot analysis of multiple miR-15 family members in ventricular lysates at different stages of post-natal cardiac development.

Online Figure III: Cardiac-specific over-expression of miR-195 is associated with perinatal cardiomyopathy in two independent founder lines. H&E-stained heart sections of two miR-195 transgenic founder lines that died at P10 and P1, respectively (A and B). Scale bar = 1mm.

Online Figure IV: βMHC-miR-195 transgenic mice develop a late-onset cardiomyopathy and die prematurely. A, Survival curve of βMHC-miR-195 transgenic (red) and wild-type (blue) mice (n=10 per group). Transgenic males and females are represented by the solid and dashed lines, respectively. **B,** H&E-stained sections of hearts from a wild-type mouse and βMHC-miR-195 transgenic mouse that died at 5 months of age. Scale bar = 2mm.

Online Figure V: Over-expression of miR-195 does not affect cell size or apoptosis in neonatal mice. A, Quantification of cell size in wild-type (WT) and βMHC-miR-195 transgenic (TG) hearts at P1. Values represent mean±SEM from 3 hearts per group (~100 cells assessed per heart). **B,** Quantification of apoptosis in WT and TG hearts at P1. Values represent the number of TUNEL positive nuclei per field. Data presented as mean±SEM from 3 hearts per group (7 fields of cells assessed per heart).

Online Figure VI: Adenoviral-directed over-expression of miR-195 in cultured neonatal cardiomyocytes induces G2 arrest and binucleation. A, Titration of adenovirus expressing miR-195 in cultured neonatal cardiomyocytes. miR-195 expression levels were determined by real-time PCR and are normalized to U6 and expressed as a fold change relative to uninfected cells. Neonatal cardiomyocytes were infected with 0, 20 or 40 ul of Ad195 to achieve expression levels comparable to endogenous miR-195 in the P14 heart (red bar). **B,** Representative images of cultured neonatal cardiomyocytes (stained with α-actinin) infected with 100 MOI of either AdGal or Ad195 for 48 hours. Arrows denote binucleate cardiomyocytes. **C,** Analysis of cell cycle progression through G1, S and G2 phases by flow cytometry in cultured neonatal cardiomyocytes over-expressing miR-195. Neonatal cardiomyocytes were infected with either Ad195 or AdGal for 48 hours. The proportion of cells in G1, S and G2 phases of the cell cycle is shown for each treatment for one representative experiment (n=3 independent experiments performed in total). **D,** Analysis of cell cycle progression through G1, S and G2 phases by flow cytometry in H9c2 cells over-expressing miR-195. The proportion of cells in G1, S and G2 phases of the cell cycle is shown for H9c2 cells infected with either AdGal or Ad195 for 48 hours.

Online Figure VII: microRNA expression profiling and RISC-sequencing of miR-195 transgenic mouse hearts. A, Pie chart showing the number of genes that were up- or down-regulated (>1.5-fold) in miR-195 transgenic cardiac ventricles at P1. **B,** Venn diagram depicting the overlap among 3 different miRNA prediction algorithms (Targetscan, miRanda, PITA) for the 39 predicted miR-15 family target genes that were down-regulated in miR-195

transgenic hearts at P1. **C,** Venn diagram showing the number of genes that were either unique or shared between miR-195 transgenic and wild-type RISComes. **D,** mRNA abundance (log_2-adjusted FPKM) in cardiac RISCome of miR-195 transgenic and wild-type mice. The best fit linear regression line is shown (y=1.0118x), along with the calculated correlation coefficient (R^2=0.8994).

Online Figure VIII: Identification of checkpoint kinase 1 (*Chek1*) as a highly conserved direct in vivo target of miR-195. A, Table of all cell cycle genes with shared ontology (identified by DAVID gene ontology cluster analysis) that are enriched in miR-195 cardiac RISComes. The fold enrichment in miR-195 transgenic RISComes is shown for each gene. Predicted miR-15 family binding sites are shown for each gene using 3 different computational algorithms for miRNA target identification (Targetscan, miRanda and PITA). Evolutionary conservation (mouse to human) for each binding site within predicted target genes is also indicated. **B,** Schematic showing mammalian conservation of the miR-195 binding site within the 3'UTR of *Chek1*.

Online Figure IX: Temporal regulation of miR-195 and *Chek1* during post-natal cardiac development. Real-time PCR analysis of miR-195 and *Chek1* mRNA expression levels over the first 56 days of post-natal life in mice. Expression levels expressed as a fold change relative to P0.

Online Figure X: Optimization of miR-15 family knockdown in neonatal mice using antimiRs directed against miR-15 and miR-16. A, Real-time PCR analysis of miR-15 family expression at P12 following subcutaneous administration (25 mg/kg each) of control oligo, anti-15, anti-16 or a combination of anti15/16 between P2-P4. Note that the combination of anti-15/16 oligos is required to knock down all miR-15 family members. **B,** Northern blot confirming knockdown of several miR-15 family members at P12. A Northern blot for let7a is also shown, demonstrating specificity of antimiR-mediated miRNA knockdown.

Online Figure XI: Post-natal inhibition of the miR-15 family is associated with an increased number of cardiomyocytes with disorganized sarcomeres. A. Sections from P12 control and anti-15/16-treated hearts stained with phospho-histone H3 (green) and cardiac troponin T (red) to label mitotic cardiomyocytes. Note cardiomyocytes in anti-15/16-treated hearts with disorganized sarcomeric structure (arrowheads), some of which stain positive for phospho-histone H3 (arrow). **B.** Quantification of the number of cardiomyocytes displaying disorganized sarcomeric structure (disassembled sarcomeres). Data presented as cells/field for n=3 independent samples per group (10 fields of cells assessed per heart). Values presented as mean±SEM, *P<0.05. **C.** Sections from P12 control and anti-15/16-treated hearts stained with wheat germ agglutinin (WGA) to label cell membranes. **D.** Quantification of cell size in control and anti-15/16-treated hearts at P12. Values represent mean±SEM from 3 hearts per group (~250 cells assessed per heart).

Online Figure XII: Analysis of non-conserved miR-195 RISC-seq 'targets' following post-natal inhibition of miR-15 family members. Real-time PCR analysis of genes containing predicted (but non-conserved) binding sites for the miR-15 family that were enriched in miR-195 RISComes at P1. Expression levels following anti-15/16 treatment for each gene are presented as a fold change relative to mice that received a control oligo. Values presented as mean±SEM, *P<0.05.

A

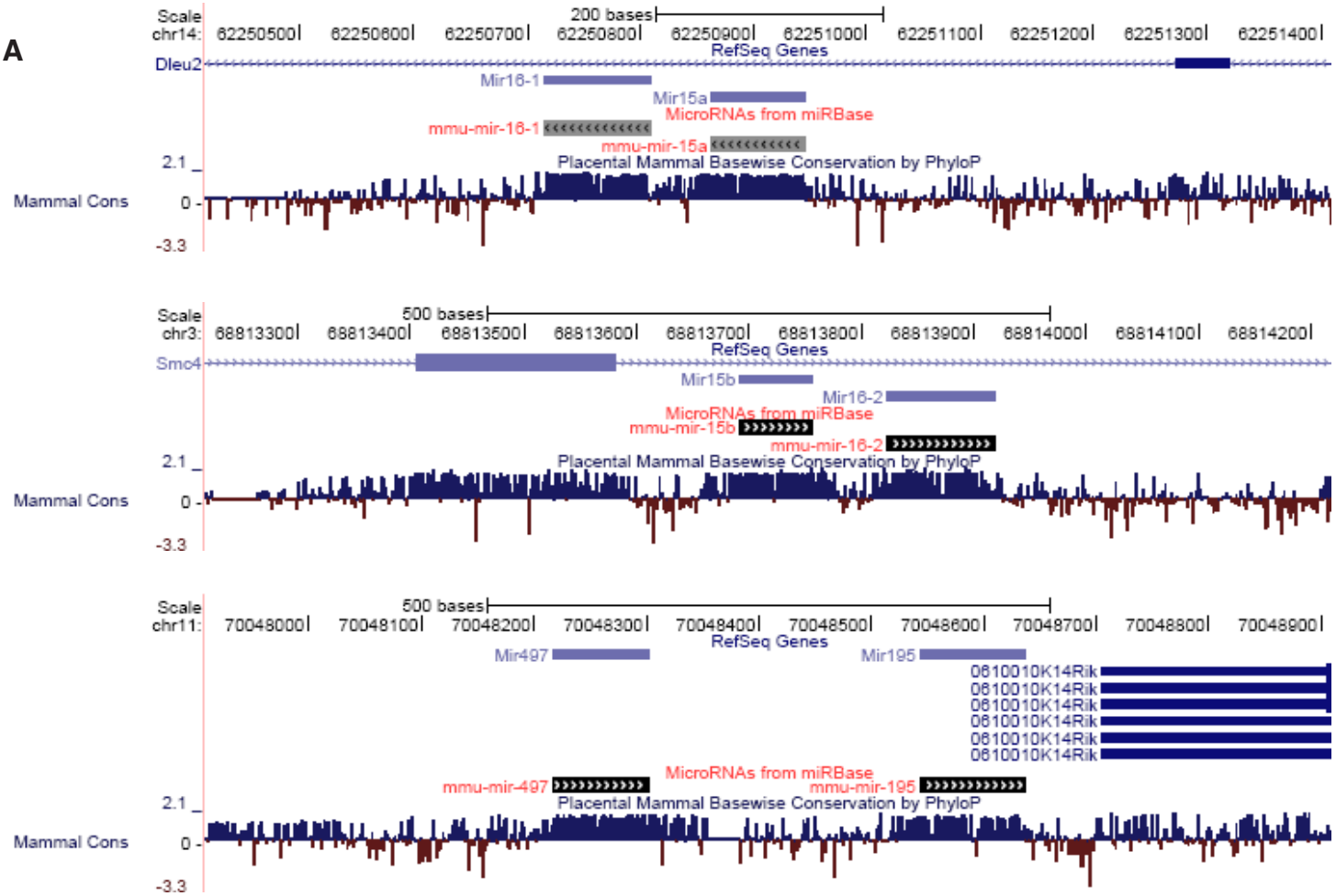

B

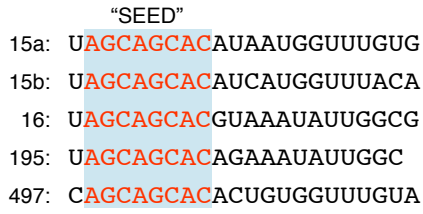

Online Figure I

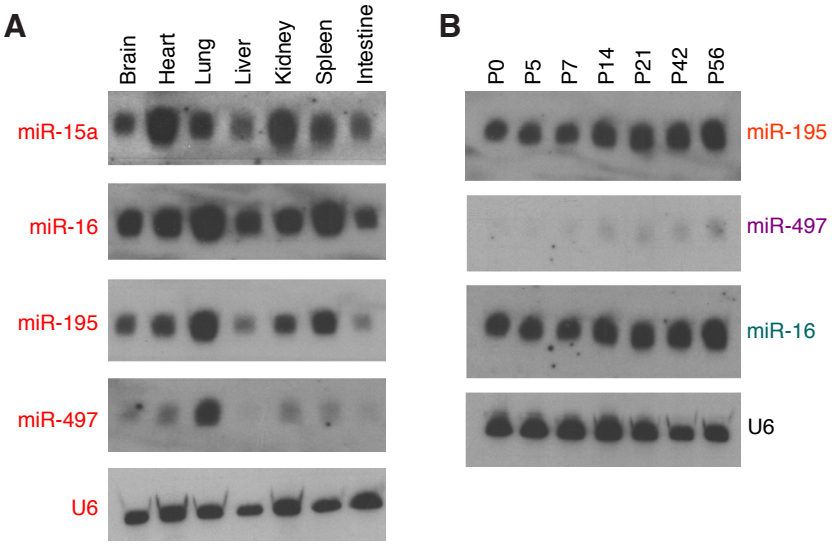

Online Figure II

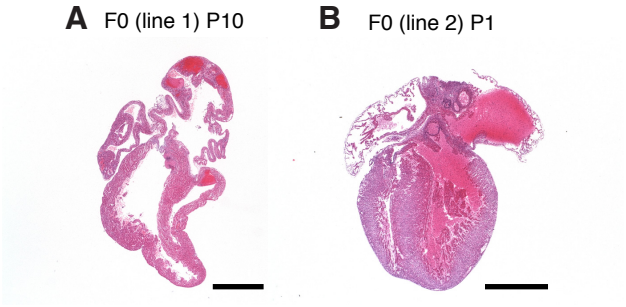

Online Figure III

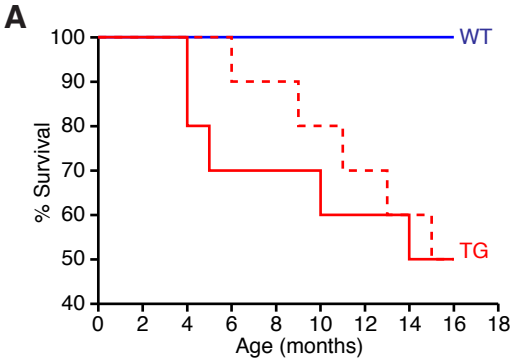

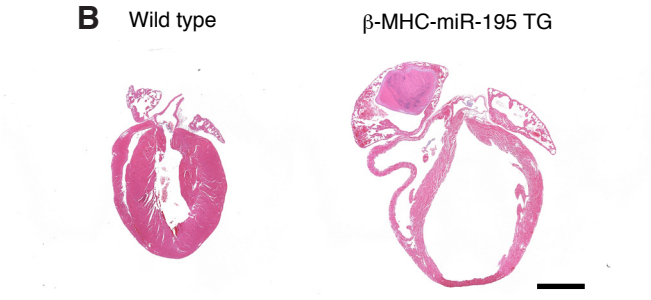

Online Figure IV

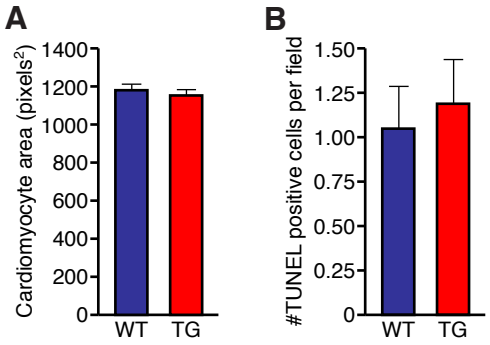

Online Figure V

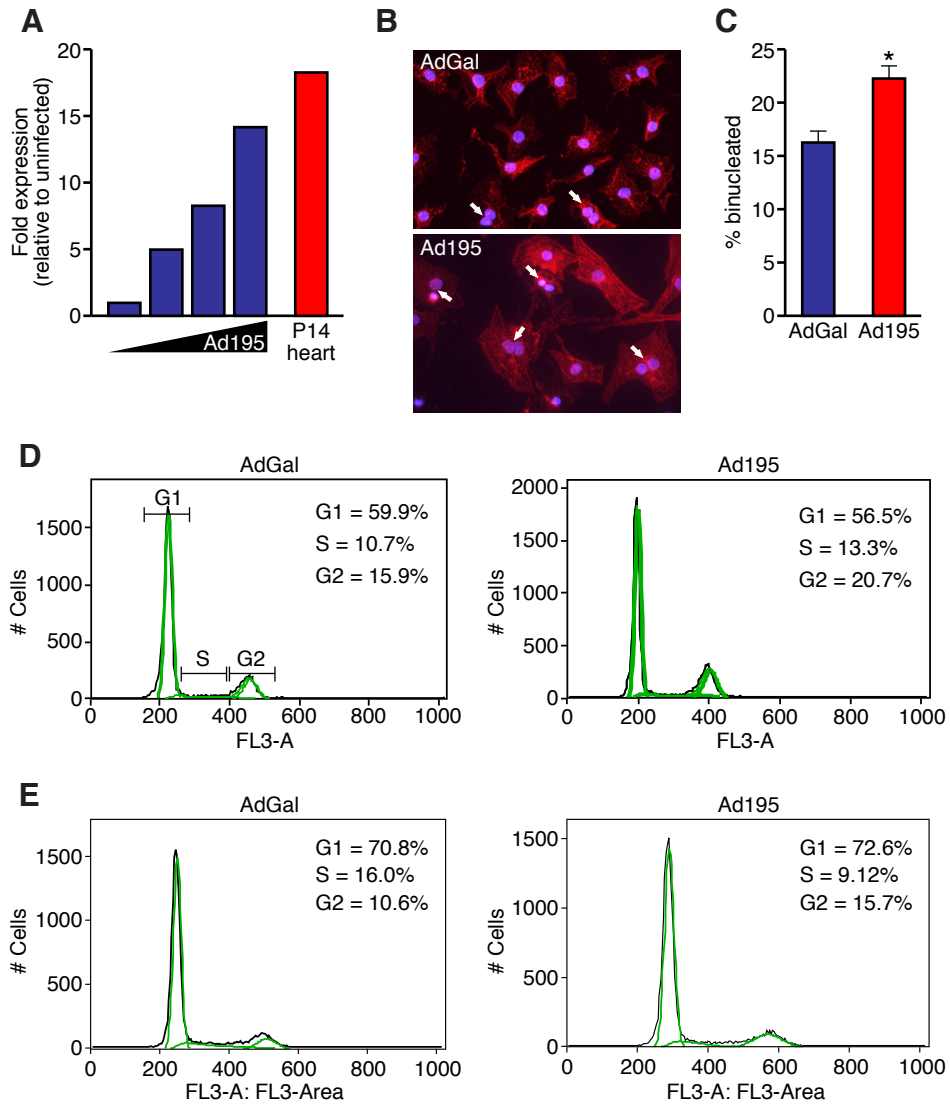

Online Figure VI

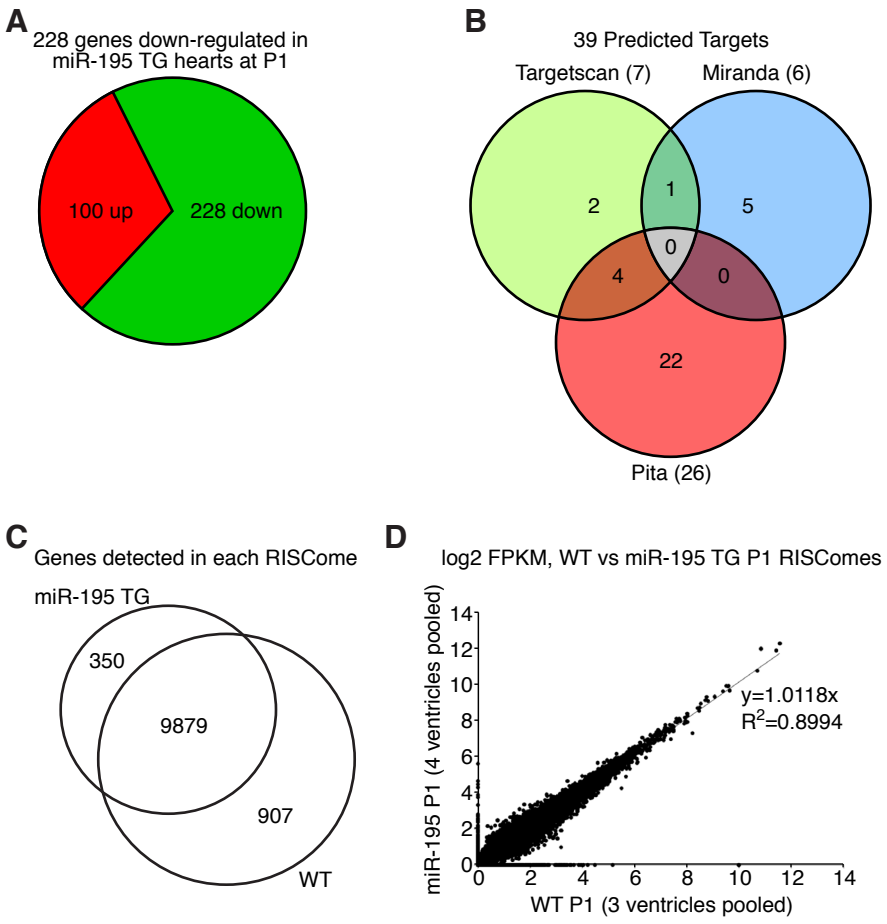

Online Figure VII

A

Gene	Fold Enrichment (TG vs. WT)	Targetscan	miRanda	Pita	Conserved Binding Site?
BIRC5	4.1			X	NO
CENPV	3.6				
TIPIN	3.3				
MAD2L1	2.9				
KIF20B	2.8				
NUP43	2.7				
E2F5	2.6				
POLA1	2.6				
CHEK1	2.6	X		X	YES
CDC2A	2.6			X	NO
CDCA8	2.4				
CENPE	2.3				
NDC80	2.3				
CCDC99	2.2				
KIF11	2.2				
LRRCC1	2.2				
NUSAP1	2.2			X	NO
SPAG5	2.1		X		NO
BUB1B	2.1				
RBBP8	2.0				

B

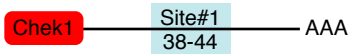

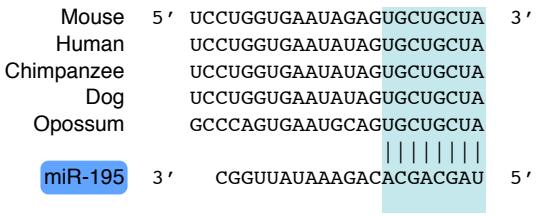

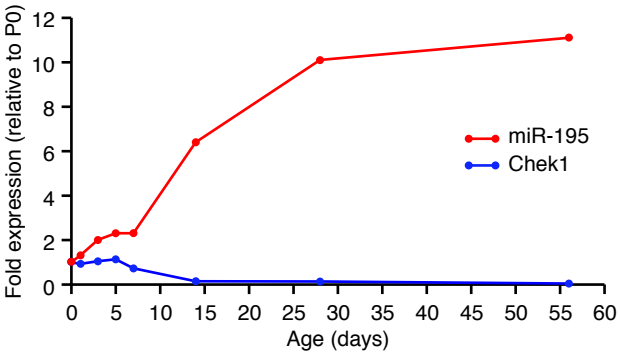

Online Figure IX

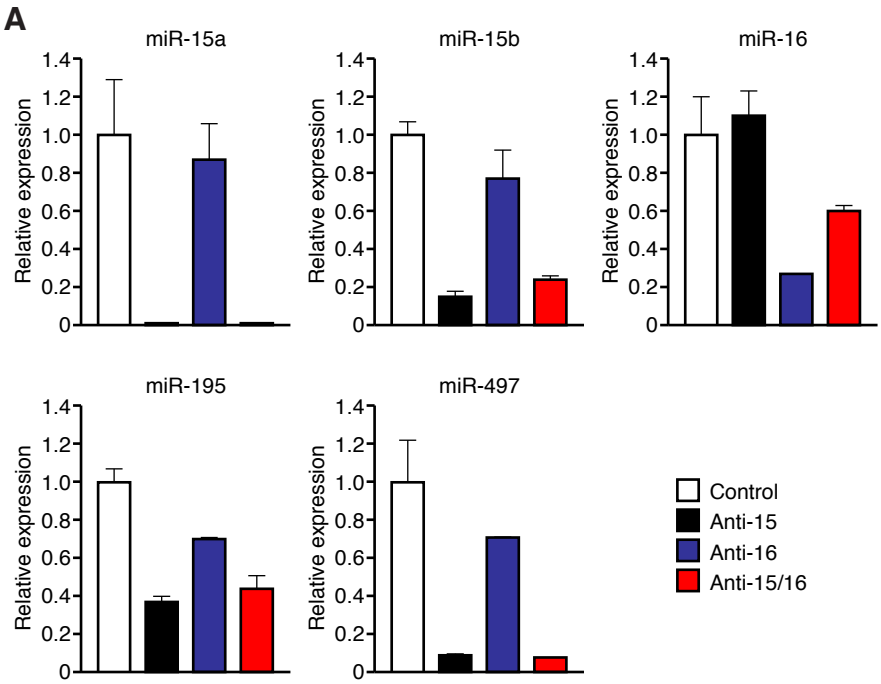

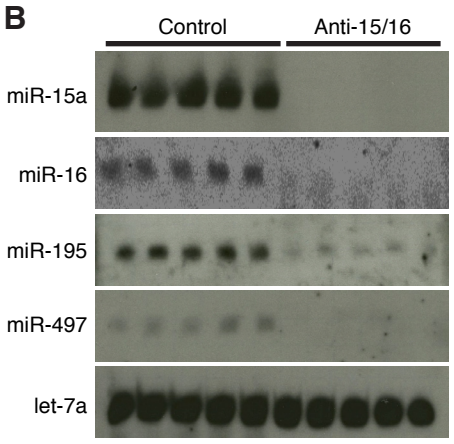

Online Figure X

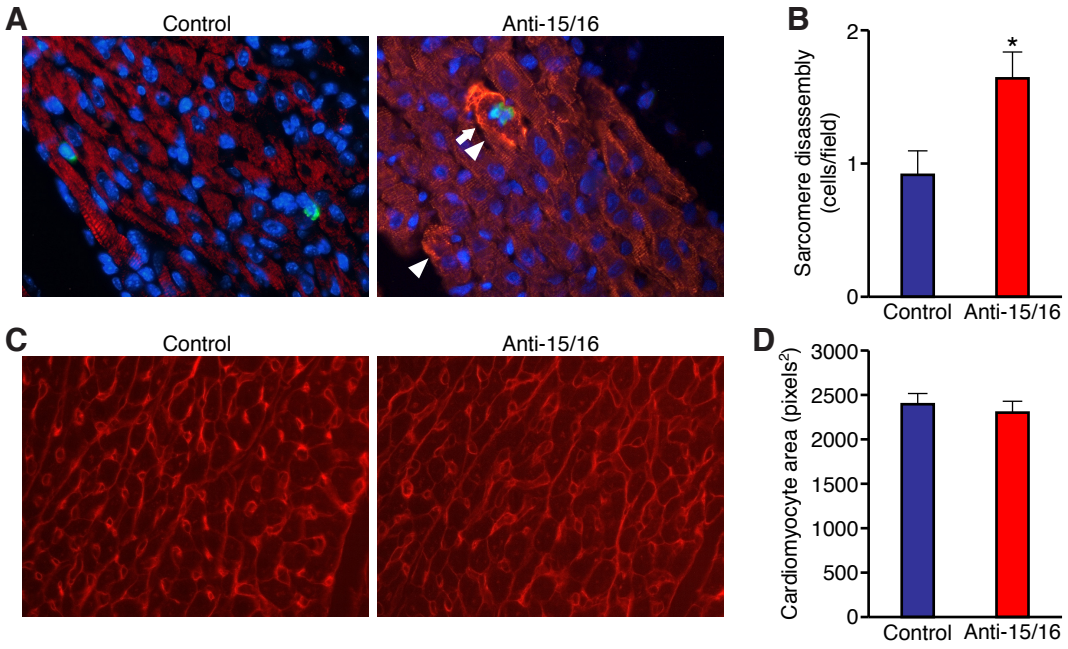

Online Figure XI

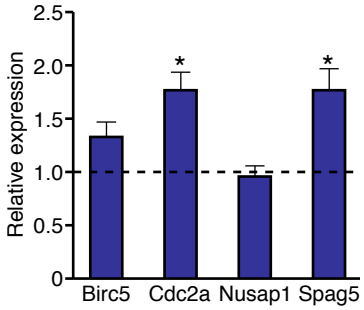

Online Figure XII